ELSEVIER

Thin-Walled Structures **24** (1996) 231–259

0263-8231/96/$15.00

0263-8231(95)00030-5

Compressive Strength of Rectangular Plates Under Biaxial Load and Lateral Pressure

C. Guedes Soares & J. M. Gordo

Unit for Marine Technology and Engineering, Instituto Superior Técnico, Universidade Técnica de Lisboa, Av. Rovisco Pais, 1096 Lisboa, Portugal

(Received 7 July 1994; accepted 20 December 1994; received for publication 8 June 1995)

ABSTRACT

Equations are derived to assess the strength of plates subjected to biaxial compressive loads, including the effect of initial distortions and residual stresses. These equations are then extended to the case of simultaneous lateral pressure loads.

In calibrating the proposed methods and in assessing their model uncertainty published results of experiments and of numerical calculations have been used.

The proposed methods were shown to be unbiased as regards plate slenderness and aspect ratio. The model uncertainty of each method was quantified and thus can be used to derive design formulations with the desired level of safety.

NOTATION

a	Plate length
b	Plate width
A	Regression coefficient
B	Regression coefficient
B_Q	Modelling factor for the effect of lateral pressure
B_r	Modelling factor for the effect of residual stresses
E	Young's modulus of elasticity
E_t	Tangent modulus of elasticity
K	Buckling coefficient

q_o	Lateral load
Q_L	Non-dimensional lateral load parameter
R	Biaxial strength
R_Q	Effect of lateral pressure
$R_{r\delta}$	Correction factor for imperfections
$R_x = \sigma_x/\sigma_{xu}$	Longitudinal strength ratio in biaxial compression
R_x^*	Percentage of longitudinal loading (eqn. 33)
$R_y = \sigma_y/\sigma_{yu}$	Transverse strength ratio in biaxial compression
t	Plate thickness
T_r	Non-dimensional residual stress ($= \sigma_r/\sigma_o$)
T_x	Non-dimensional longitudinal stress ($= \sigma_x/\sigma_o$)
T_y	Non-dimensional transverse stress ($= \sigma_y/\sigma_o$)
$\alpha = a/b$	Aspect ratio
$\beta = b/t\sqrt{\sigma_o/E}$	Plate slenderness
$\delta = \omega_1/t$	Non-dimensional amplitude of distortions
η	Width of the weld induced zone of residual stresses
$\Delta\phi_b$	Reduction of plate strength due to residual stresses
ϕ_x	Longitudinal strength
ϕ_{xr}	Longitudinal strength of plates with residual stresses
ϕ_{xu}	Longitudinal ultimate strength
ϕ_y	Transverse strength ϕ_{ym} strength of the midfield of a plate loaded transversely (eqn (8))
ϕ_{yu}	Ultimate transverse strength
γ	Strength parameter (eqn (9))
ν	Poisson coefficient
ψ	Coefficient accounting for nonuniform load distribution (eqn (13))
σ_{cr}	Critical stress
σ_e	Buckling stress
σ_o	Yield stress
σ_r	Residual stress
σ_x	Longitudinal stress
σ_{xu}	Ultimate longitudinal stress
σ_y	Transverse stress
σ_{yu}	Ultimate transverse stress

1 INTRODUCTION

There are many studies available concerning the compressive strength of plate elements and of stiffened panels. There are also several simplified design equations that have been proposed along the years. The various

proposals have been based on different assumptions which implies that their accuracy will depend on the situation to which they are applied, as indicated in Ref. 1.

Most of the design equations were concerned with the uniaxial strength, both in the longitudinal[2–4] or in the transverse direction.[5,6] However some studies have addressed the strength of biaxially loaded plates[7–10] which is the objective of the present study.

There is a significant amount of data that has become available recently, both from tests and from numerical studies. These results are particularly useful to understand the effects of weld-induced initial distortions and residual stresses, of the plate aspect ratio, and of combined loading. Therefore, it is timely to review the existing results and to reassess the existing design methods, so as to propose improvements, which is the purpose of the present paper.

This paper will consider the biaxial compressive strength and after reviewing the existing formulations and results a new strength assessment method is derived. The influence of residual stresses and initial imperfections is assessed and the model uncertainty of the formulation is quantified.

Plates under biaxial load and lateral pressure are also studied and it is shown that lateral pressure decreases significantly the strength of the plates. A new strength assessment method is proposed and its model uncertainty is assessed.

In designing plate elements it is desirable to introduce a safety coefficient which ensures that the plate will resist the largest loads expected to occur during its lifetime. This safety coefficient will therefore depend not only on the variability of the load but also of the strength assessment.

The components of uncertainty in a strength assessment method are not only the variability of the basic variables, but also of the model itself.

The simplified models as the ones considered in this paper only account explicitly for the most significant variables, which means that one should expect some scatter from their predictions.

The systematic deviations and the scatter of the predictions of a model can be assessed by introducing a model uncertainty factor.[11,12] The statistical description of this factor can be derived from comparisons of experimental and numerical results. The mean value will indicate the systematic deviation, which can be used to correct the formula on an average sense, and the standard deviation will quantify the uncertainty.

The safety factors that will change a strength assessment method into a design method will be proportional to that uncertainty and they can be derived as described in Refs 13 and 14 for the case of plates under uniaxial compressive loads.

2 PLATE ELEMENTS UNDER BIAXIAL LOADING

2.1 Existing formulations

Different proposals have been put forward to model the collapse of plates that result from the interaction between longitudinal and transverse stresses in a manner that is suitable for design in general and for code specifications in particular.[7] The approach that has been generally adopted consists in predicting the longitudinal and the transverse stresses in a plate as a function of plate slenderness and of other parameters like aspect ratio and eventually initial defects. The equivalent stress in the plate is determined from a combination of the stress components. Thus, interaction curves have been proposed to combine the non-dimensional longitudinal stress ratio $R_x = \sigma_x/\sigma_{xu}$ with the non-dimensional transverse stress ratio $R_y = \sigma_y/\sigma_{yu}$ where the subscript u indicates ultimate strength.

It should be noticed that different formulations of σ_{xu} and σ_{yu} have been advanced by the authors that have proposed the interaction curves. Thus each of the stress ratios R_x and R_y indicated hereafter should be referred to the original author's formulations of longitudinal and of transverse strength, i.e., $R_x = T_x/\phi_{xu}$ and $R_y = T_y/\phi_{yu}$, where $T_x = \sigma_x/\sigma_o$ and $T_y = \sigma_y/\sigma_o$.

One expression that has been used in the Det norske Veritas (DnV) rules, American Bureau of Shipping (ABS) rules and in the British Standard BS.5400 is the quadratic interaction:

$$R_x^2 + R_y^2 = 1 \tag{1}$$

which represents a circle in the $R_x - R_y$ plane. DnV proposed as normalising strengths the Faulkner's formula[2] in the longitudinal direction and the one of Valsgard[5] in the transverse direction, which are respectively:

$$\phi_{xu} = \frac{2}{\beta} - \frac{1}{\beta^2} \text{ for } \beta \geqslant 1 \tag{2a}$$

$$\phi_{xu} = 1 \text{ for } \beta \leqslant 1 \tag{2b}$$

and:

$$\phi_{yu} = \frac{\phi_{xu}}{\alpha} + 0{\cdot}08 \cdot \left(1 + \frac{1}{\beta^2}\right)^2 \cdot \left(1 - \frac{1}{\alpha}\right) \tag{3}$$

where ϕ_{xu} is given by eqn (2), α is the plate aspect ratio and β its slenderness. The rules of the American Bureau of Shipping (ABS) use the same interaction formula but with different normalising strengths. They prefer to use a formulation based on the Bryan elastic buckling stress combined

with the Johnson–Ostenfeld approach to account for the effect of plastic deformation. The buckling strength σ_{cr} of a plate is equal to the elastic buckling strength σ_e:

$$\frac{\sigma_e}{\sigma_o} = \frac{\pi^2}{12(1-\nu^2)} \frac{K}{\beta^2} \text{ for } \sigma_e \leqslant 0{\cdot}5\,\sigma_o \tag{4}$$

when buckling occurs in the elastic range i.e. when $\sigma_e \leqslant 0{\cdot}5\,\sigma_o$. The Poisson's ratio ν is 0·3 for steel plates and the buckling coefficient K accounts for the type of loading and of boundary conditions. For a wide plate with linearly varying transverse loading it is given by Ref. 15:

$$K = \left(1 + \frac{1}{\alpha^2}\right)^2 \frac{2{\cdot}1}{\psi + 1{\cdot}1} \text{ for } 0 \leqslant \psi \leqslant 1 \tag{5}$$

where the factor is such that when the stresses on one transverse edge of the plate are σ on the other one they are $\psi \cdot \sigma$. Thus for plates under uniform compressive stresses $\psi = 1$. For longitudinal loading with uniform applied stresses ($\psi = 1$) K becomes equal to 4.

When the predicted strength is greater than half the yield stress, the collapse strength is given by:

$$\frac{\sigma_{cr}}{\sigma_o} = 1 - \frac{1}{4}\frac{\sigma_o}{\sigma_e} \text{ for } \sigma_e > 0{\cdot}5\,\sigma_o \tag{6}$$

which implies an elasto-plastic collapse.

However, other authors have proposed parabolic curves, as for example Faulkner *et al.*:[7]

$$R_x + R_y^2 = 1 \tag{7}$$

In this case the ultimate transverse strength should be computed by the expression of the same authors:[7]

$$\phi_{yu} = \frac{0{\cdot}9}{\beta^2} + \frac{1{\cdot}9}{\beta\alpha} \cdot \left(1 - \frac{0{\cdot}9}{\beta^2}\right) \tag{8}$$

Valsgard[9] generalised this expression by including cross terms and making the exponent of R_x a variable γ:

$$R_x^{\gamma} - \eta R_x R_y + R_y^2 \leqslant 1 \tag{9}$$

where $\eta \geqslant 0$ is a constant. The proposed normalising equations are (2) and (3), respectively for the longitudinal and transverse directions. On the basis of his numerical results on a plate with aspect ratio of 3, Valsgard proposed the following design curve:

$$R_x - 0{\cdot}25 R_x R_y + R_y^2 \leqslant 1 \tag{10}$$

which corresponds in fact to $\gamma = 1$ and $\eta = 0{\cdot}25$.

Dier and Dowling[16] have considered a more comprehensive treatment which would also be applicable to cases in which one of the load components was tensile. This implies that they are considering the interaction curve not only in the first quadrant of the $R_x - R_y$ plane (biaxial compression), but also in the others (biaxial tension). They proposed:

$$R_x^2 + 0{\cdot}45 R_x R_y + R_y^2 = 1 \tag{11}$$

which includes a positive contribution of the cross terms.

In view of all the uncertainty of the results and the different interaction curves available, Stonor *et al.*[17] proposed a lower bound curve to the existing data, which turned out to be:

$$R_x^{1{\cdot}5} + R_y^{1{\cdot}5} = 1 \tag{12}$$

Very stocky plates should behave according to the von Mises equation, which was generalised in terms of the ultimate directional stress instead of the yield stress:

$$R_x^2 - R_x R_y + R_y^2 = 1 \tag{13}$$

The choice of adequate normalising equations, ϕ_{xu} and ϕ_{yu}, should make eqn (13) an upper bound curve.

Figure 1 shows a comparison between some of the various interaction curves referred.

2.2 Existing results

Becker and associates[18, 19] have conducted a series of tests on steel plates under biaxial compression. The specimens were small square tubes of 0·64 mm thick mild steel to AISI standard 1010 or of 0·76 mm stainless steel 4130. The specimens were electron beam-welded and in some cases they have been stress-relieved. The tubes were loaded longitudinally by applying loads to their ends and transversely by applying four equal inward loads along the corners of the tube. Thus, each specimen provides information about four plates.

In the first series of tests the conditions for combined loading were different from the ones of only transverse loading. The longitudinal load was applied through stiff plates which restrained the out-of-plane displacements of each plate element. However, in the tests with only transverse loading, the ends of the tube could slide over the platens and no effective restrain existed then. The transverse loading frame applied the load to two

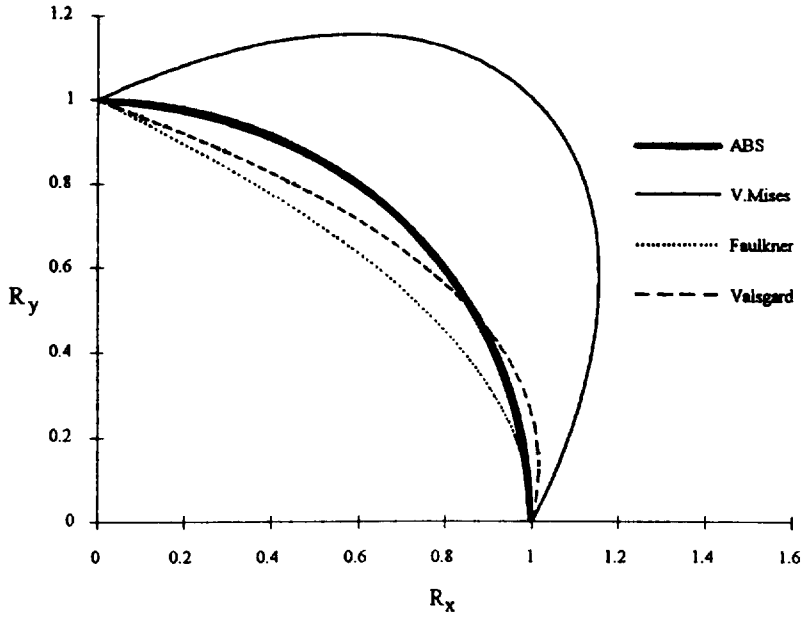

Fig. 1. Comparison between different interaction curves for biaxial compression.

opposed corners of the tube and the adjacent corners would react against the fixed frame.

In the second series of tests the longitudinal loads were applied similarly. However, end plates were fitted in the tube to maintain the shape of the ends when only transverse loading was applied. This second series of tests was performed largely on high strength stainless steel which did not have a distinct yield point. The results were non-dimensionalised with respect to the 0·2% proof stress, which is not clearly the correct parameter to use.

The tests of Stonor *et al.*[17] were aimed at studying the overall behaviour of the plates loaded biaxially, by measuring the longitudinal load-shortening curve for each plate. Out-of-plane deflection measurements were made to identify the mode in which the plate failed.

The major attention was concentrated on the maximum load supported by the plate. Most tests were performed under constant transverse loading but some were performed under proportional loading to allow assessment of the effects of different loading paths. The loading consisted of a dominant longitudinal compression together with a small transverse compressive loading. Thus, the failure mode was expected to be a limited modification of the uniaxial loading case.

Plates of aspect ratio 4 and 6 were tested. The longitudinal loading generated higher stresses and was applied to the shorter pair of edges of length b. The transverse loading was a constant force per unit length applied over the centre portion of the longer edges, over a length of $2b$ and $4b$. The uniformity of the stresses in the central loaded portion of the plate was tested by comparing results for plates with aspect ratios of 4 and 6, maintaining all other parameters equal.

The transverse loading was constant along the loaded portion of the longitudinal edge. This precludes the operation in the post-buckling regime where transverse loading is mainly carried in two zones adjacent to each loaded end, with considerably smaller transverse stresses in the central part of the plate. This is different from the conditions of longitudinal edges remaining straight.

The longitudinal load was applied through a stiff wedge-jack, a set of discrete fingers were used to restrain the out-of-plane displacements of the longitudinal edges. They were flexible in the x and y directions to avoid the transfer of the longitudinal loads into their supports and to allow inward and outward in-plane movement of the longitudinal edges. Only simply supported tests were conducted.

Longitudinal residual stresses were introduced by beads of weld metal laid parallel to and close to the longitudinal edges. It was considered that not enough was known about the distribution of transverse residual stresses for it to be possible to simulate them in the tests. Initial out-of-flatness was introduced by using an hydraulic jack carrying a small cap as load spreader. After the spring back the remaining deflection had the shape of a sine wave.

The tests were performed on 6 mm steel plates complying with BS 4360, Grade 50B. All plates failed by the formation of a single large buckle at the centre, corresponding to the position of the initial dent. In the plates of $b/t = 35$ the buckle length is similar to the plate width but for b/t of 45 and 55 this length grew to $1{\cdot}3b$.

Dowling *et al.*[8] presented results of numerical predictions of the biaxial strength of plates with slenderness ranging between 20 and 120, with an aspect ratio of 3:1 and with varying levels of initial distortions and residual stresses.

All the results relate to mild steel plates and the geometric imperfections have a single wave and a three wave component, the ratio of which is fixed. The average level was considered to have as amplitudes of the first and third modes $\delta_{01} = 0{\cdot}1\beta^2$ and $\delta_{03} = 0{\cdot}05\beta^2$. Slight and severe distortions were also considered. The results were used to assess one proposal of interaction equation for the longitudinal and transverse stresses.

2.3 Analysis of results

The results used in this study include 233 numerical predictions of Dowling *et al.*[8] the two experimental series of Becker *et al.*[18,19] with 18 and 8 points, the 16 tests of Stonor *et al.*[17] and the 110 tests of Dier and Dowling,[16] in a total of 385 data points.

The available results have been plotted in Fig. 2 as a function of the non-dimensional longitudinal and transversal stresses, normalised by the yield stress of the material. The slendernesses of the plates are identified by a number such that

$$\beta = i \text{ when } i - 0{\cdot}5 \leqslant \beta < 1 + 0{\cdot}5$$

This figure shows a very large spread of results and the only tendency that is clear is the fact that with increasing slenderness the results approach the origin.

A significant improvement is obtained if one uses the theoretical collapse strength in each direction as the normalising factor instead of the yield stress. Figure 3 shows the plot of the results when the longitudinal

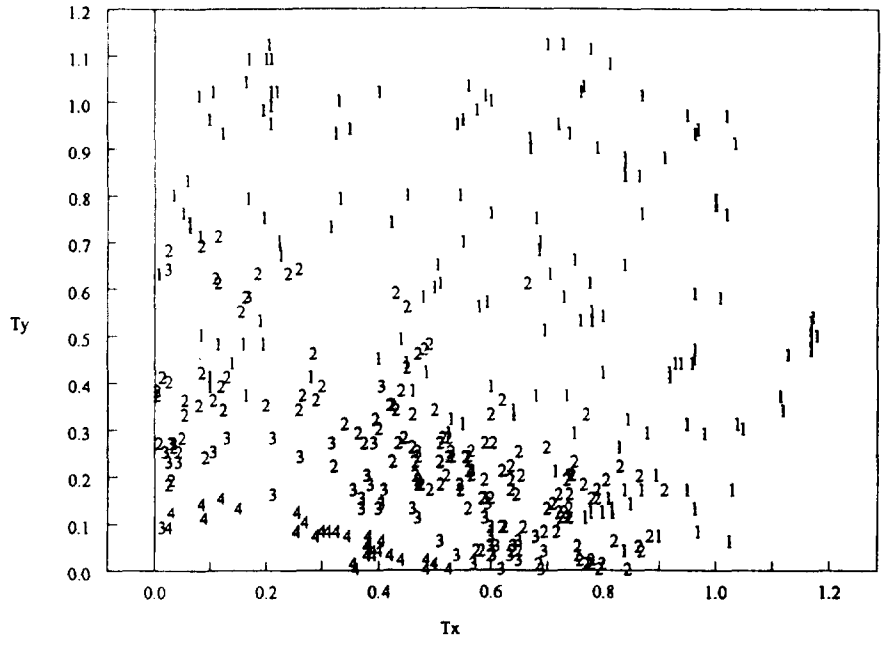

Fig. 2. Experimental and numerical results as a function of longitudinal and transverse stresses normalised by the yield stress. The members at the data points indicate the slenderness of the plate.

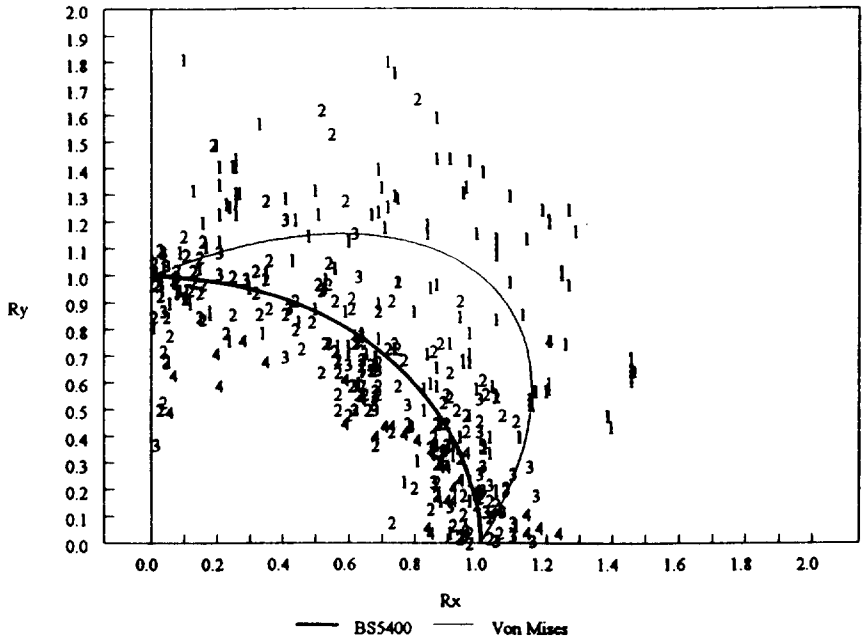

Fig. 3. Results with the applied stresses normalised respectively by the longitudinal and transverse strength predictions, for all slenderness ratios, showing also eqn (1) and the Von Mises criterion.

stresses are divided by eqn (2) and the transverse stresses by eqn (3), indicating a clear decrease in the spreading of the results.

One aspect that results from that plot and which is worth commenting on is the series of results obtained for a value of R_x close to zero, which lie well below one. Whenever $R_x = 0$ one has pure transverse loading in which case the plates have a different mode of collapse and a lower strength.[6] These results reflect exactly this change in mode of collapse with its weakening effect.

Another feature worth comment is the fact that for almost uniaxial longitudinal loading several plates show a strength 10% larger than the yield stress. This effect had already been noted in uniaxially loaded plates in the stocky end, as discussed for example in Ref. 4.

It is common to use as a normalising yield stress the one obtained from tension tests because this is the material property that most commonly characterises the material. However, the compression yield stress is normally 5%–10% larger and if this value was adopted, the results would lie closer to the curve.

The very stocky plates with $\beta < 1{\cdot}0$ fail in general by plastic collapse

without any buckling weakening effect. In these cases the boundary restraint of having the edges straight develops bidimensional effects that may even increase the plate strength. The strength curves are less applicable in this region and for example the Faulkner uniaxial strength equation (eqn 2(a)) is valid only for $\beta > 1{\cdot}0$. Separating the points in the data base which have $\beta < 1{\cdot}5$ from the others identifies the two different types of behaviour as shown in Fig. 4. Figure 5 resumes the results obtained for each interaction curve and should provide the basis to further development.

Figure 4 shows the interaction curve proposed in British Standard BS5400 (eqn (1)) as well as Von Mises yield criterion defined in respect to the ultimate stresses instead of the yield stress as usual. It can be observed that for stocky plates ($\beta \approx 1$) the Von Mises curve is closer to the results than the interaction curve even though in this case many of the results are still outside the curve. Figure 4 shows that this curve could be used to predict those results.

The agreement with the Von Mises curve is not surprising because stocky plates will fail basically in a plastic collapse governed by the equivalent yield stress, since no buckling mechanism is present. If one

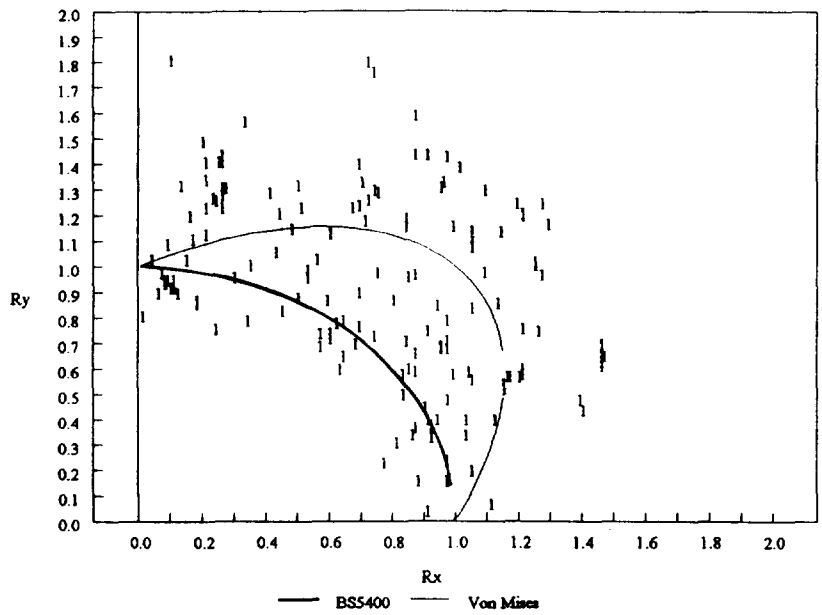

Fig. 4. Results with the applied stresses normalised respectively by the longitudinal and transverse strength predictions, for $\beta < 1{\cdot}5$, showing also eqn (1) and Von Mises curve.

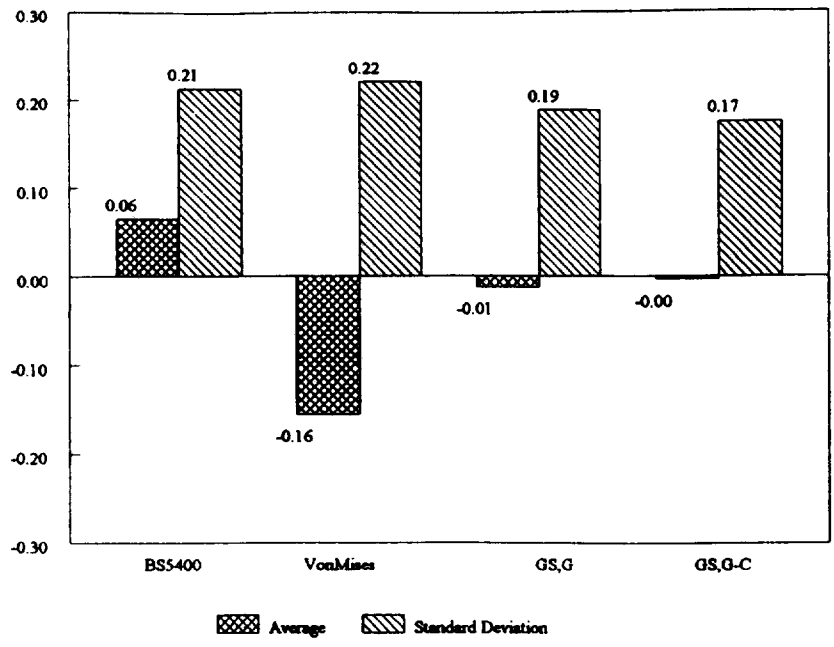

Fig. 5. Mean value and standard deviation of the modelling variable for the various interaction equations.

assumes that these plates will have their strength described by the Von Mises curve the other plates in the data base will be much closer to the BS5400 interaction curve.

The bias of the different interaction curves is quantified as the distance between the point and the interaction curve in the $R_x - R_y$ plane. For the ABS formulation (BS 5400) it resulted in a bias of 0·06 and a standard deviation of 0·21, as indicated in Fig. 5.

With the present suggestion of using the Von Mises curve for the stocky plates and the circle (eqn (1)) for the others, the bias was reduced from 0·06 to −0·01 and the standard deviation to 0·19 as also indicated in the same figure under GS,G.

Although the method proposed gives good results, an inspection of Fig. 4 shows that there are a large number of plates with a transverse strength larger than the critical stress but on the order of magnitude of the yield stress. Those plates have a slenderness smaller than 1·3 which leads to the hypothesis that in the biaxial loading of the stocky plates with $\alpha \neq 1$, there is an interaction between the longitudinal and transverse collapse modes leading to an increased ultimate transverse strength.

Since in these cases the collapse mode is closer to the one of a plate with

longitudinal compression, it is proposed to assess their strength by the longitudinal strength formula (eqn (2)) instead of the transverse one (eqn (3)). Applying this method, the standard deviation which was 0·22 for the Von Mises curve is reduced to 0·18 for the stocky plates. Therefore this is considered as the best procedure to predict the strength of biaxially loaded plates.

The results indicated in Fig. 5 as GS,G were obtained from prediction equations that do not account for the effect of residual stresses. However, in the tests of Becker the plates had residual stresses, which were induced during the fabrication of the tubes. These longitudinal residual stresses can be accounted for by reducing the predictions of eqn (2) accordingly, before one uses it in defining R_x.

The longitudinal residual stresses σ_r in a rectangular plate are given by:

$$\frac{\sigma_r}{\sigma_o} = \frac{2\eta}{(b/t) - 2\eta} \tag{14}$$

where ηt is the width of the yield tension zone at the edges of the plate. The strength reduction due to these residual stresses can be represented by the multiplicative factor B_r:

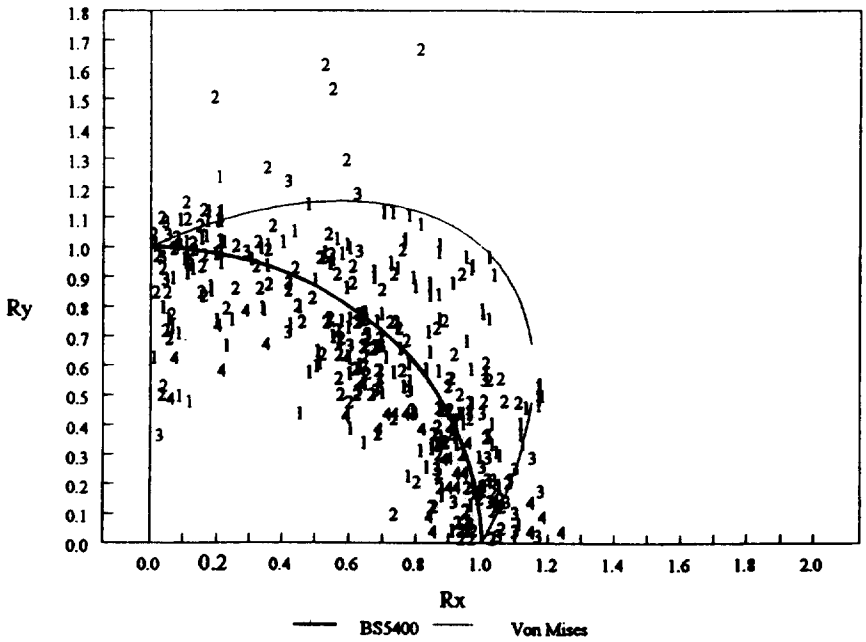

Fig. 6. Results with the transverse stress normalised by the transverse strength when $\beta > 1{\cdot}3$ and by the longitudinal strength when $\beta < 1{\cdot}3$, which is the final proposal.

$$B_r = 1 - \Delta\sigma_b = 1 - \frac{\sigma_r}{\sigma_o}\frac{E_t}{E} \tag{15}$$

where the effects of plastic deformations are accounted for by the tangent modulus of elasticity E_t, which is given by Ref. 20:

$$\frac{E_t}{E} = \frac{\beta - 1}{1{\cdot}5} \text{ for } 1 \leqslant \beta \leqslant 2{\cdot}5 \tag{16a}$$

$$\frac{E_t}{E} = 1 \text{ for } \beta \geqslant 2{\cdot}5 \tag{16b}$$

in a more simplified version of the formula given in Ref. 2.

Now the strength of plates with longitudinal residual stresses ϕ_{xr} can be predicted as:

$$\phi_{xr} = \phi_x B_r \tag{17}$$

Valsgard's method can also account explicitly for the level of residual stresses. This is accomplished in the way R_x is defined in eqn (1). Instead of being given by eqn (2), which is valid for the case of no residual stresses, it becomes:

$$\phi_{xr} = \frac{1{\cdot}8}{\beta} - \frac{0{\cdot}8}{\beta^2} \quad (\beta \geqslant 1) \tag{18}$$

In principle, in the method proposed here the effects of residual stresses could also be accounted for in the same way. However, the results in Fig. 5 indicate that the residual error before accounting for initial defects is already very small. Thus it was chosen to perform a regression of those errors on the levels of residual stresses and initial distortions so as to define a correction factor $R_{r\delta}$ that would modify eqn (1) to become:

$$R_x^2 + R_y^2 = R_{r\delta}^2 \tag{19}$$

The analysis of all the data lead to the following regression:

$$R_{r\delta} = 1{\cdot}13 - 0{\cdot}42\, T_r - 0{\cdot}08\, \delta \tag{20}$$

where $T_r = \sigma_r/\sigma_o$ is the non dimensional residual stress ratio and δ is the amplitude of the initial distortions. Using eqns (19) and (20) instead of eqn (1) to predict the plate strength an improvement is obtained in the standard deviation of the residuals, which decreases from 0·19 to 0·17, as indicated in Fig. 5 under GS,G-C. One has to note that the first result (GS,G) was obtained using the Von Mises equation for plates with $\beta < 1{\cdot}3$ while the circular interaction was used for all slendernesses in GS,G-C, but normalising the transverse stress of the stocky plates with the longitudinal ultimate strength, eqn (2).

The previous discussion has indicated that the plate behaviour was different for plates in the stocky range ($\beta < 1{\cdot}3$) and in the slender zone ($\beta > 1{\cdot}3$). In the first case the collapse is basically plastic, and thus the residual stresses are less important than the initial distortions. The contrary happens for slender plates which fail in the elastic and elasto-plastic regime. This is clearly shown in the results when performing the regression on the two data sets:

$$R_{r\delta} = 1{\cdot}11 - 0{\cdot}16T_r - 2{\cdot}01\delta + 0{\cdot}27R_x^*, \quad \beta < 1{\cdot}3 \tag{21a}$$

$$R_{r\delta} = 1{\cdot}12 - 0{\cdot}58T_r - 0{\cdot}07\delta + 0{\cdot}04R_x^*, \quad \beta > 1{\cdot}3 \tag{21b}$$

where R_x^* is a percentage measure of the longitudinal loading:

$$R_x^* = R_x \Big/ \sqrt{R_x^2 + R_y^2} \tag{21c}$$

which appears to have an influence in stocky plates but seems to be of no importance for slender plates, as is inferred from the coefficients of eqn (21).

If one now uses eqns (19) and (21) instead of eqn (1), the standard deviation of the errors comes down from 0·19 to 0·13, which is very satisfactory as a model uncertainty of a design method. Figure 7 shows the plot of the results after the correction has been applied and it can be observed that a relatively small spreading is apparent.

The residual errors have been plotted in Fig. 8 as a function of plate slenderness, showing that they are not dependent on β. Figure 9 shows a similar plot in which the residuals are shown as a function of the percentage of longitudinal load R_x^* showing again that no bias exists.

Another check that has been made is the effect of the plate aspect ratio on the results. Table 1 shows a summary of the results indicating that no major differences exists for the bias in each group of α.

A slight tendency may be present, with the bias changing from −8% for $\alpha = 1$ to 5% for $\alpha = 5$ or 6 but the effect is not worth accounting for. The standard deviation is larger for $\alpha = 3$, but this is probably the result of having results from various different sources in that case, which brings an additional source of variability.

Finally the results have been grouped by author, as indicated in Table 2. Its inspection shows that the results of Becker have the largest mean error and standard deviation. This is possibly the result of various factors among which are the fact that the test series was made in small specimens and that they had different initial distortions. However, although the results of Becker have these larger values, they are not significantly different from the others, which indicates that the results have good consistency despite being from several origins.

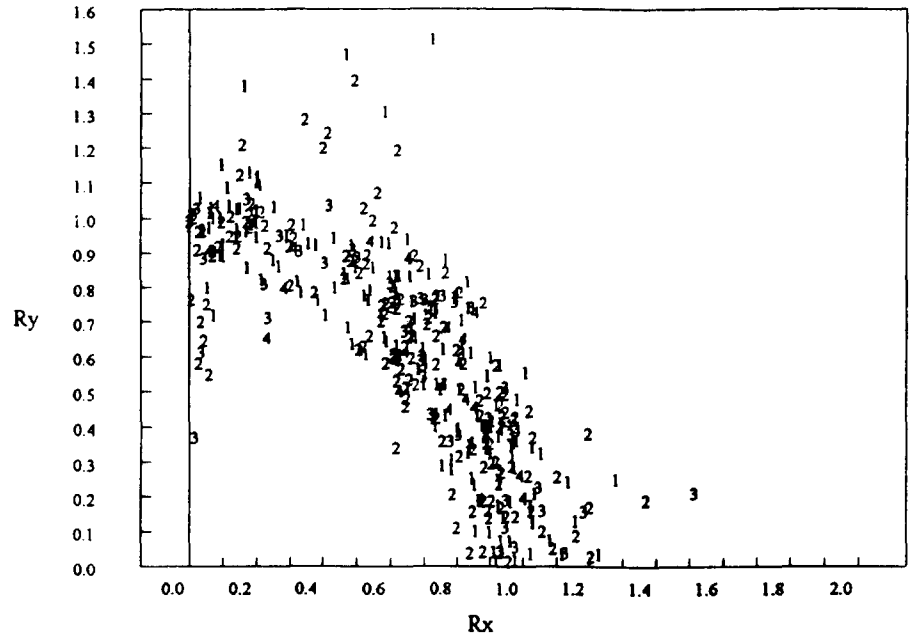

Fig. 7. Results with the applied stress normalised by the present proposal corrected for the effects of residual stresses.

Figure 10 shows the relative occurrence of deviations of the experimental and numerical points from the interaction curves in the plane of R_x and R_y, as shown in Figs 1 and 9. The results have been obtained for the various proposals of interaction curves and it is apparent that the present proposal (GS,G) leads to a stronger concentration around the value of 0·0.

To assess the performance of eqns (19) and (21), a model error B_{xy} can be defined as:

$$\sqrt{R_x^2 + R_y^2} - R_{r\delta} = B_{xy} \tag{22}$$

For an unbiased formula this quantity should have a mean value of zero and to improve the precision of the formula, the standard deviation should be as small as possible. Table 3 summarises the characteristics of this parameter as calculated from the numerical data in the case of the ABS formulation (eqns (1), (4) and (6)), Faulkner formulation (eqns (2), (7) and (8)), and the present one (eqns (2), (3), (19) and (21)). It is shown that the present formulation is an unbiased one and that the standard deviation is significantly decreased compared with the two others.

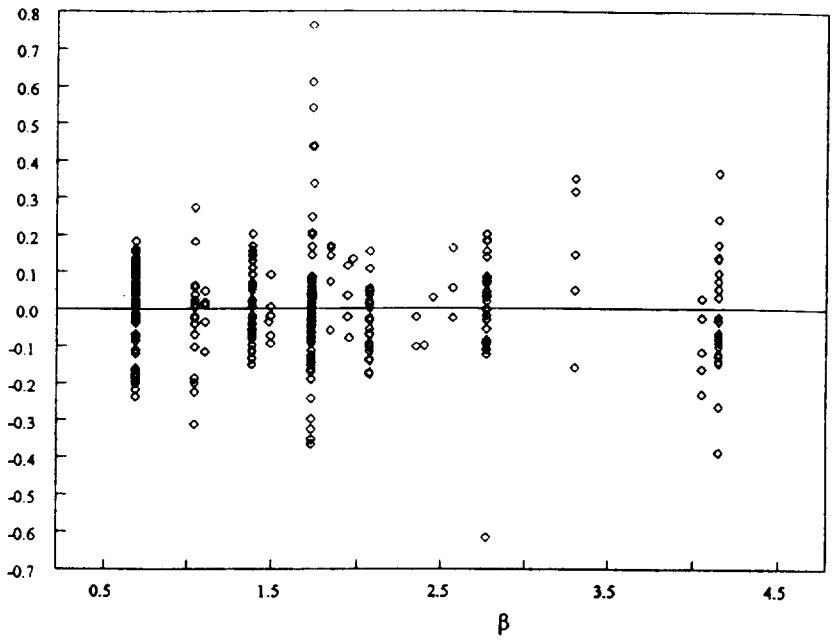

Fig. 8. Deviation of the results from the proposed interaction curve, as a function of slenderness, after applying the corrections for the residual stresses.

TABLE 1
Statistics of the Residual Errors as a Function of the Plate Aspect Ratio

α	n	*AVG*	*STD*
1	42	−0·08	0·06
2	3	−0·02	0·03
3	320	0·01	0·14
4	14	−0·02	0·07
5	4	0·06	0·03
6	2	0·04	0·05
All	385	−0·00	0·13

3 BIAXIAL LOADING AND LATERAL PRESSURE

In general, lateral pressure on panels causes out-of-plane displacements in a mode that is one half wave in both directions. These out-of-plane deflections will decrease the plate strength whenever they coincide with the

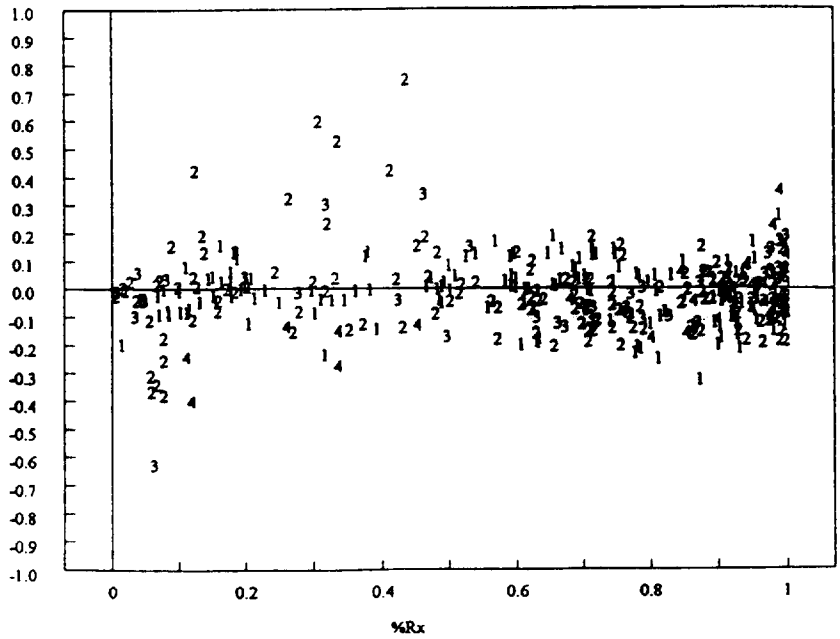

Fig. 9. Deviation of the results from the proposed interaction curve, as a function of the level of longitudinal loading, after applying the corrections for the residual stresses.

TABLE 2
Statistics of the Residuals for the Data of Each Author, Indicating Whether the Results are Numerical (N) or Experimental (E)

Reference	*n*	*AVG*	*STD*
Dowling (1979) (N)	233	−0·01	0·15
Becker (1970) (E)	18	0·07	0·13
Stonor (1983) (E)	16	−0·01	0·07
Becker (1977) (E)	8	0·04	0·22
Dier (1980) (N)	110	−0·01	0·09
All	285	−0·00	0·13

main buckling mode and they will increase the plate strength otherwise. Thus, in the case of biaxial strength of long panels, that type of deflection tends to decrease the transverse strength and to increase the longitudinal strength, the net effect depending on the specific situation.

There are not many publications dealing with this complicated problem, although one is able to find some analytical, numerical and experimental

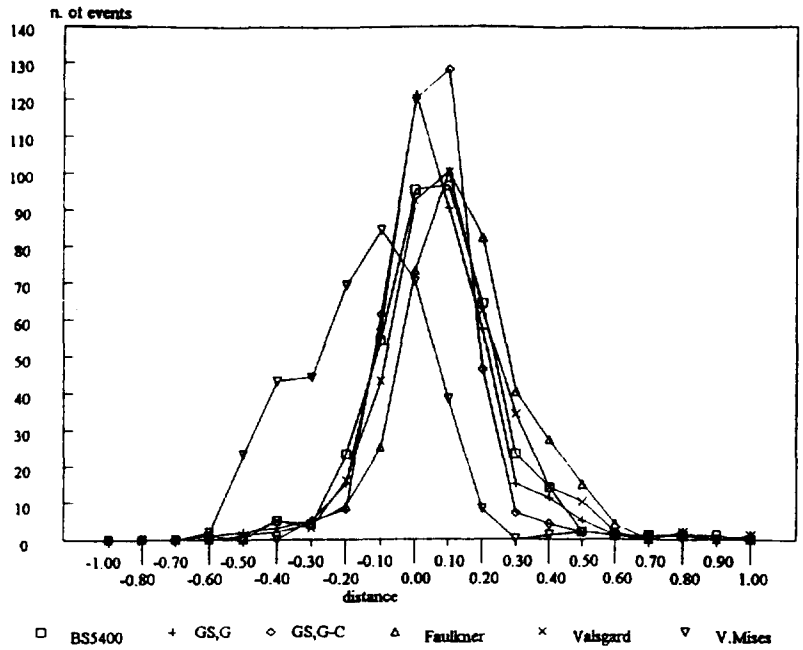

Fig. 10. Relative frequency of the deviation distance of the results from the interaction curves for different proposals.

TABLE 3
Statistics of the Residuals from the Different Methods

	ABS	*Faulkner*	*GS,G*
AVG	0·21	−0·06	0·00
COV	0·31	0·24	0·13

results in the literature. Steen and Valsgard[10] presented a design method for plates subjected to biaxial compression and lateral pressure, which was based on deriving simplified non-linear elastic response curves for the in-plane and laterally loaded cases and combining the local stresses obtained into an equivalent stress criterion. The elastic buckling and the initial postbuckling behaviour of plates was described by the perturbation theory of Budiansky,[21] which is based on the non-linear Von Karman equations and includes the effect of geometrical imperfections. The non-linear elastic behaviour of the plate under lateral load was then addressed. The stresses corresponding to both types of behaviour are assessed and combined in a Von Mises equivalent stress which is used as a criterion for the initial yield

and the ultimate collapse load. Interaction curves are provided for square plates of different slenderness and degree of initial imperfection.

Dier and Dowling[16] conducted an extensive numerical study dealing with plates with an aspect ratio of 3 and with square plates with simply supported and fully clamped boundary conditions. The plates had b/t ratios of 40, 60 and 80 and different levels of initial imperfections and residual stresses. The results were obtained for different levels of lateral pressure and they were shown in the form of interaction curves.

Experimental results are also scarce. Becker *et al.*[22] conducted some tests on the square tubes that were described previously. Now transverse load was also applied as well as internal pressure. Further experimental results were presented by Yoshiki *et al.*[23] Yamamoto *et al.*[24] and Okada *et al.*,[25] although all of them are of plates under uniaxial load and lateral pressure.

In general the experimental and the numerical results allow one to say that the transverse strength of the plates is significantly affected by lateral pressure, while the effect on the longitudinal strength is small. The lateral pressure has also an effect of decreasing the sensitivity of plate strength to initial imperfections.

Dier and Dowling[12] have proposed that the lateral pressure could be represented by a non-dimensional parameter:

$$Q_L = q_o E/\sigma_o^2 \tag{23}$$

where q_o is the intensity of the lateral pressure. On the other hand, all the Japanese authors use an alternative formulation:

$$Q_{LJ} = \frac{q_o b^4}{Et^4} = Q_L \beta^4 \tag{24}$$

which includes also some information on plate geometry. The first formulation was adopted here because it is independent of the plate geometry.

The data available consists of 373 points which have been plotted in Fig.18 where both the longitudinal and transverse stresses have been normalised by the yield strength i.e. $T_x = \sigma_x/\sigma_o$ and $T_y = \sigma_y/\sigma_o$. The large scatter that is apparent was slightly reduced in Fig. 19 when the results were normalised by the strength predictions of biaxially loaded plates without lateral pressure (eqn (1)).

An inspection of the results allows one to conclude that the lateral load induces significant degradation of strength, which is dependent on the load intensity and on the plate slenderness. Thus a formulation that accounts explicitly for those effects is required. The effect of the lateral pressure was accounted by including an additional term R_Q to the inter-

action equation used for the biaxial load (eqn (1)). Different options have been considered and the one finally adopted has the form:

$$R - R_Q = 0 \tag{25a}$$

where

$$R^2 = R_x^2 + R_y^2 \tag{25b}$$

The effect of the lateral pressure was modelled by a regression equation, dependent both on Q_L and on β. Different types of relations were tested and the one which showed best results was of the form:

$$R_Q = A - BQ_L\beta^2 \tag{26}$$

where A and B are regression coefficients.

The results of the regression on the various sources of data are summarised in Table 4 which indicates that for all data, the effect of lateral pressure can be summarised as:

$$R_Q = 1.0 - 0{\cdot}116Q_L\beta^2 \tag{27}$$

which should be introduced in eqn (25) to give the interaction equation for biaxially loaded plates with lateral pressure. As indicated in Table 4 this equation has a correlation coefficient, ρ, of 0·65 and the standard deviation of the errors is 0·16.

As shown in Figs 11 and 12 some of the data points had one of the load components in tension, despite the fact that most of them had both in compression. If one uses only the points corresponding to biaxial compression, their number reduces to 235 but eqn (27) is almost unchanged. In fact, the regression coefficient changes from 0·116 to 0·117, the

TABLE 4

Regression Coefficients of eqn (25), Correlation Coefficient (ρ) and Standard Deviation (std) for Various Data Sets and Summary of All Data (373) and of the Ones Only in Compression (235)

Author	*Load*	*n*	*A*	*B*	*ρ*	*std*
Dier	Biaxial	235	0·99	0·112	0·82	0·11
Yoshiki	Uniaxial	25	1·09	0·153	0·58	0·09
Yamamoto	Uniaxial	23	0·90	0·112	0·84	0·06
Okada	Uniaxial	18	1·19	−0·030	0·18	0·07
Becker	Biaxial	72	0·90	0·010	0·04	0·23
All	—	373	1·00	0·116	0·65	0·16
Compression		235	1·00	0·117	0·75	0·14

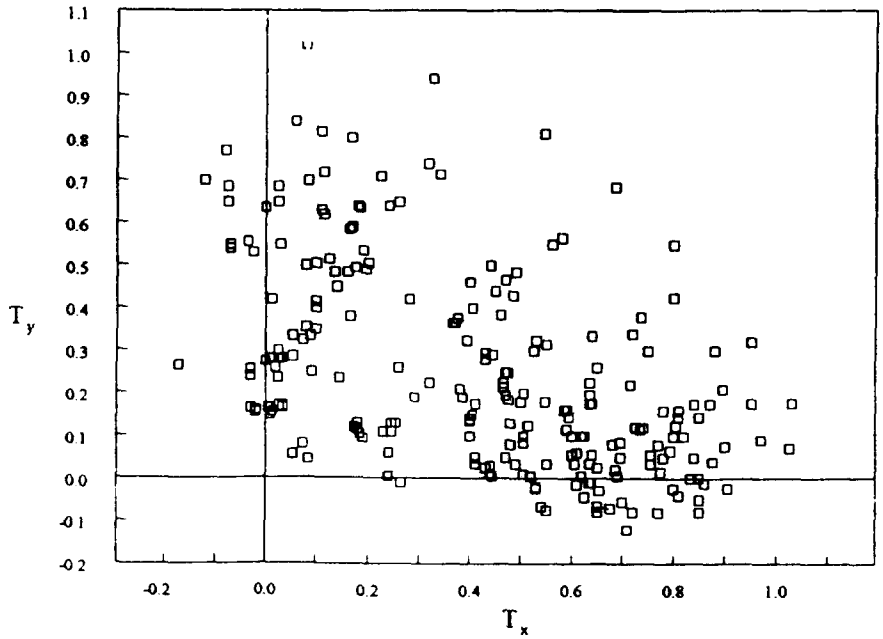

Fig. 11. Numerical and experimental results of plates subjected to biaxial load and lateral pressure normalised by the yield stress.

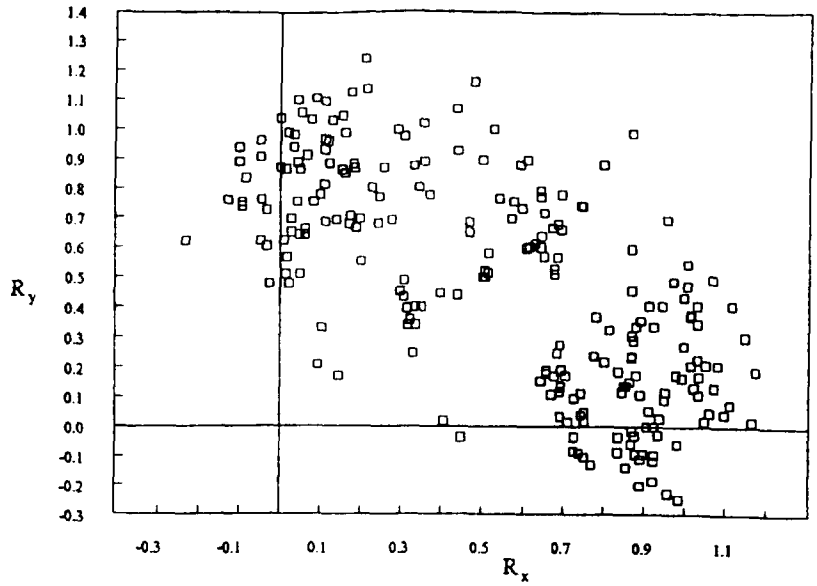

Fig. 12. Numerical and experimental results of plates subjected to biaxial load and lateral pressure normalised by the predictions of the strength of biaxially loaded plates without account of lateral pressure.

correlation coefficient increases from 0·65 to 0·75 and the standard deviation of the errors decreases from 0·16 to 0·14.

Table 4 shows that in general the effect of lateral pressure represented by the regression coefficient B varies somewhat from author to author. In the data from Yoshiki *et al.*[19] a significantly larger effect of the lateral pressure is indicated in the larger regression coefficient (0·153). The data from Okada *et al.*[21] show a negative coefficient indicating that the plates would become stronger with $Q_L\beta^2$, which seems surprising. Finally Becker *et al.* have conducted two series of tests in 1970 and 1977. If the two sets of data are treated separately one obtains 0·08 and 0·02 for the coefficient B which is 0·01 for all data. Thus one can see that there are some differences between the experimental data although the numerical results of Dier and Dowling[12] and the experimental ones of Yamamoto *et al.*[20] are in agreement.

At any rate the numerical data of Dier and Dowling[12] is more consistent than the experimental one and is equally spread in the $R_x - R_y$ plane, as shown in Fig. 13. Figure 14 shows all data after the corrections of eqns (25) and (27) are applied. It is apparent that the spreading increases only slightly, but it is greater for pure longitudinal loading ($R_y = 0$) or pure transverse loading ($R_x = 0$) combined with lateral pressure.

Table 5 presents a numerical summary of the results of applying eqn (25)

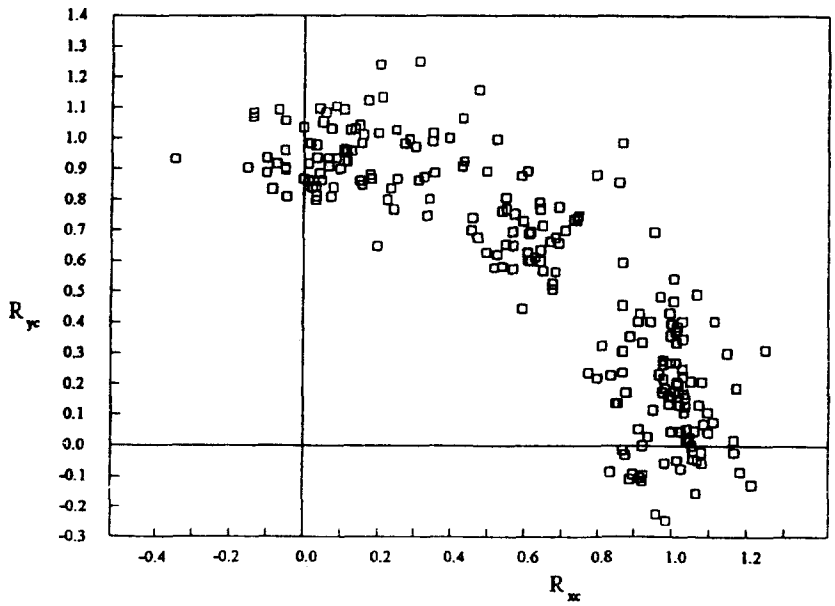

Fig. 13. Numerical results of plates with biaxial load and lateral pressure corrected for the effect of lateral pressure.

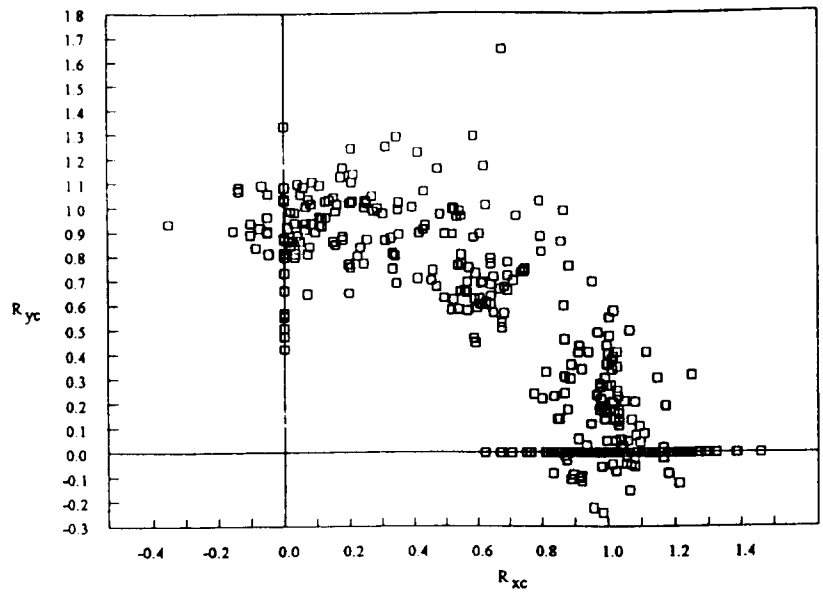

Fig. 14. Experimental and numerical results of the collapse of plates with biaxial load and lateral pressure.

to the data. In fact, it shows the statistics of the modelling factor B_Q defined as:

$$B_Q = R + R_Q \tag{28}$$

which is plotted in Fig. 15. The mean values that are indicated correspond to the right hand side of eqn (25a) which are only 1·0 when the lateral pressure correction is introduced. There is a difference of 11% from accounting for lateral pressure. The standard deviation of the residuals is reduced from 0·21 to 0·16, but the improvement in the coefficient of variation is even greater, from 0·23 to 0·16.

It is apparent from comparing Fig. 12 with Fig. 14 that the results for plates without transverse load have a larger variability than the ones with transverse load. Although the transverse loading is an additional factor that could bring additional variability, it finishes up having a stabilising effect and decreasing the variability of the results.

The residual of eqn (26) are shown in Fig. 16 as a function of the parameter $Q_L\beta^2$, indicating clearly that there exists no bias, and thus that eqn (28) is adequate to describe the influence of lateral pressure.

It has been investigated if the plate aspect ratio has any influence in the results. Table 6 summarises the mean value and standard deviation of the

TABLE 5

Statistics of the Model Factor B_Q When the Data is Normalised by the Yield Stress (T), by the Biaxial Strength (R) or with the Present Proposal to Account for Lateral Load ($R + R_Q$)

Author	*Load*	*n*	*Mean*			*Std deviation*			*Coef. var.*		
			T	R	$R + R_Q$	T	R	$R + R_Q$	T	R	$R + R_Q$
Dier	B	235	0·57	0·86	0·99	0·22	0·19	0·11	0·38	0·23	0·11
Yoshiki	U	25	0·62	1·01	1·07	0·11	0·10	0·09	0·18	0·10	0·08
Yamamoto	U	23	0·42	0·77	0·90	0·07	0·10	0·06	0·16	0·13	0·06
Okada	U	18	0·68	1·21	1·26	0·07	0·07	0·09	0·10	0·06	0·07
Becker	B	72	0·44	0·90	0·95	0·23	0·22	0·24	0·52	0·25	0·25
All	—	373	0·55	0·89	1·00	0·21	0·21	0·16	0·39	0·23	0·16

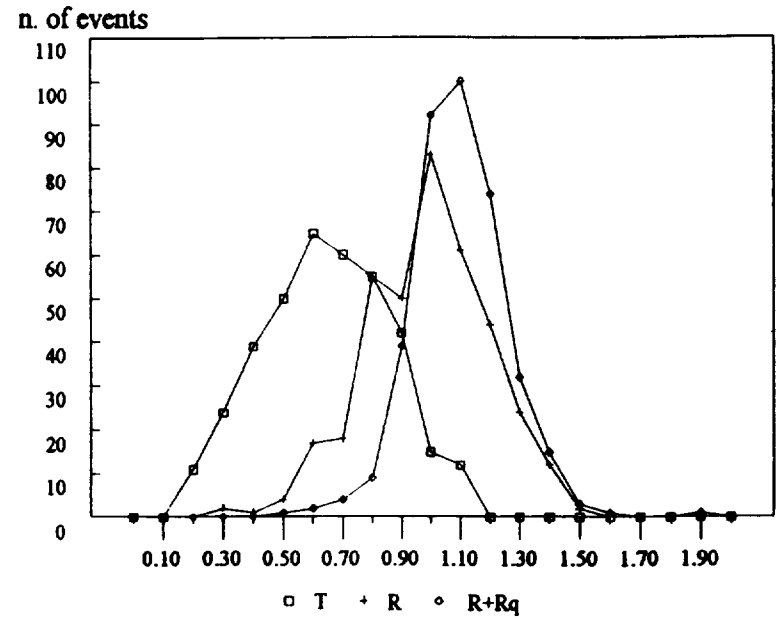

Fig. 15. Relative frequency of the deviation of the numerical results from the interaction curve proposed.

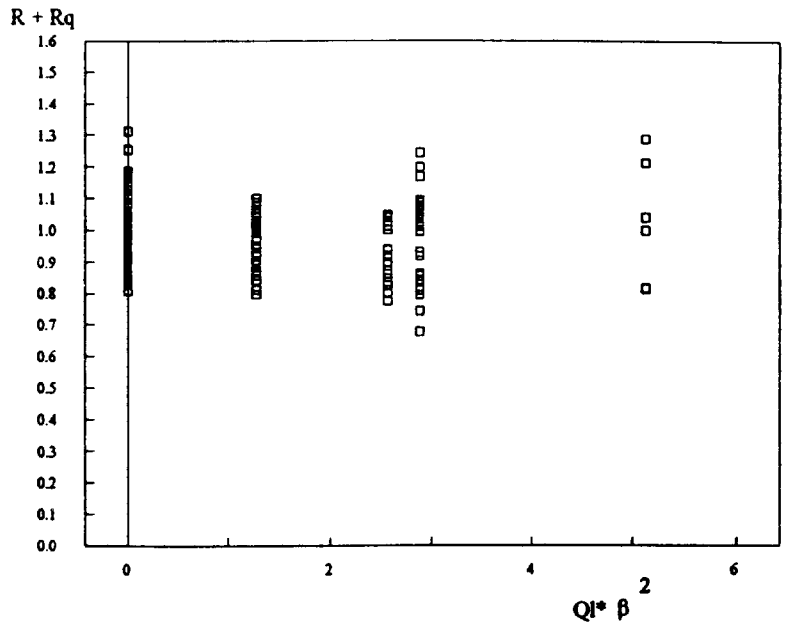

Fig. 16. Residuals of the numerical results of plates under biaxial compression and lateral load as a function of plate slenderness and load parameter.

TABLE 6
Mean Value of the Model Factor B_Q for Different Sets of Data, Function of α and of the Longitudinal Residual Stresses, σ_{rx}

α	σ_{rx}/σ_0				n	*Mean*	*Std*
	—	*0·05*	*0·20*	*0·40*			
1		1·05	0·95	0·94	89	0·99	0·10
2	1·07		0·99		33	1·05	0·09
3	0·93	1·05	0·99	0·93	234	0·98	0·17
4	1·27				9	1·27	0·11
5			0·96		8	0·96	0·15
all	1·00	1·05	0·98	0·94	373	1·00	0·16

errors after applying eqns (26) and (28) grouped in classes of different aspect ratio, no significant differences between classes have been verified in the effect of the residual stresses. Table 6 shows also the mean value of the residuals as a function of the level of residual stresses. It can be observed that there is a tendency for this value to decrease with the residual stresses but, since the value is not very large, it has not been accounted explicitly in this formulation.

4 CONCLUDING REMARKS

A survey has been provided of the available results concerning the collapse strength of rectangular plates under combined in-plane compression including the effect of lateral loading. These results were used as a basis to derive strength assessment formulas.

These equations, which are basically interaction relations between the effects of the various simultaneous loads, predict the average collapse strength of the plate element and are thus strength assessment formulations.

The method proposed here for the assessment of the strength of plate under biaxial load builds upon the interaction eqn (1), which is already adopted in existing codes like for example the British Standard, Det Norske Veritas and the American Bureau of Shipping.

However, it is proposed here that the formula should only be used for plates with $\beta > 1{\cdot}3$ and that for stockier plates the von Mises equation is adopted.

The proposed method was further extended to account explicitly for the effect of initial defects, as given by eqns (18)–(20). It was shown that the

results of this method are not dependent on the plate slenderness or aspect ratio.

The effect of lateral pressure was accounted for by extending the interaction eqn (1) and the calibration with data led to the proposal of eqns (25)–(27). These equations were shown to perform well for different aspect ratios and it was concluded that it was not necessary to account explicitly for the residual stresses.

The strength assessment methods proposed were shown to be unbiased and to have a satisfactory model uncertainty level, with values on the order of 15% which are very difficult to improve for the case of combined loads.

ACKNOWLEDGMENT

The authors express their appreciation to the American Bureau of Shipping for having sponsored this research work.

REFERENCES

1. Guedes Soares, C. & Soreide, T. H., Behaviour and design of stiffened plates under predominantly compressive compressive loads. *Int. Shipbuilding Progr.*, **30**(341) (1983) 13–27.
2. Faulkner, D., A review of effective plating for use in the analysis of stiffened plating in bending and compression. *J. Ship Res.*, **19** (1975) 1–17.
3. Guedes Soares, C., Probabilistic analysis of flat compression members. *Proc. Adv. Seminar on Structural Reliability*, CEC Joint Research Centre, ISPRA Establishment, Italy, 11–15 May, 1987.
4. Guedes Soares, C., Design equation for the compressive strength of unstiffened plate elements with initial imperfections.' *J. Constructional Steel Res.*, **9** (1988) 287–310.
5. Valsgard, S., Ultimate capacity of plates in transverse compression. *Report 79-104*, Det norske Veritas, 1979.
6. Guedes Soares, C. & Gordo, J. M., Compressive strength of rectangular plates under transverse loading. *J. Construction Steel Res.*, **16** (1995) (in press).
7. Faulkner, D., Adamschak, J. C., Snyder, G. J. & Vetter, M. F., Synthesis of welded grillages to withstand compression and normal loads. *Comput. & Struct.*, **3** (1973) 221–46.
8. Dowling, P. J., Harding, J. E. & Slatford, J. E., Plates in biaxial compression — final report. *CESLIC Rep SP4*, Dep. Civil Engng, Imperial College of Science and Technology, 1979.
9. Valsgard, S., Numerical design prediction of the capacity of plates in in-plane compression. *Comput. & Struct.*, **12** (1980) 729–39.
10. Steen, E. & Valsgard, S., Simplified buckling strength criteria for plates subjected to biaxial compression and lateral pressure. *Ship Struct. Symp. '84*, SNAME, 1984, pp. 251–72.

11. Guedes Soares, C., Uncertainty modelling in plate buckling. *Structural Safety* **5** (1988) 17–34.
12. Faulkner, D., Guedes Soares, C. & Warwick, D. M., Modelling requirements for structural design and assessment. *Integrity of Offshore Structures — 3*, eds. D. Faulkner, M. J. Cowling & A. Incecik. Elsevier Applied Science, London, 1987, pp. 25–54.
13. Guedes Soares, C., A code requirement for the strength of plate elements. *Mar. Struct.*, **1**(1) (1988) 71–80.
14. Guedes Soares, C., Design equation for ship plate elements under uniaxial compression. *J. Constructional Steel Res.*, **22** (1992) 99–114.
15. Bleich, F., *Buckling Strength of Metal Structures*. McGraw-Hill, New York, 1952.
16. Dier, A. F. & Dowling, P. J., Plates under combined lateral loading and biaxial compression, *CESLIC Report SP8*, Imperial College, Dept of Civil Engng, London, 1980.
17. Stonor, R. W. P., Bradfield, C. D., Moxham, K. E. & Dwight, J. B., Tests on plates under biaxial compression, *Report CUED/D-Struct/TR98*, Cambridge University, Engineering Department, 1983.
18. Becker, H., *et al.*, Compressive strength of ship hull girders. Part I. Unstiffened plates. *Report SSC-217*. Ship Structure Committee, Washington, DC, 1970.
19. Becker, H., Instability strength of poliaxially-loaded plates and relation to design. *Steel Plated Structures*, eds P. J. Dowling, *et al.* Crosby, Lockwood and Staples, London, 1977, pp. 559–80.
20. Guedes Soares, C. & Faulkner, D., Probabilistic modelling of the effect of initial imperfections on the compressive strength of rectangular plates. *Proc. 3rd Int. Symp. on Practical Design of Ships and Mobile Units (PRADS)*, Trondheim, Vol. 2, 1987, pp. 783–95.
21. Budiansky, B., Theory of buckling and post-buckling of elastic structures. *Advances in Applied Mechanics*, Vol. 14, Academic Press, 1974.
22. Becker, H. & Colao, A., Compressive strength of ship hull girders. Part III. Theory and additional experiments. *Report SSC-267*. Ship Structure Committee, Washington, DC, 1977.
23. Yoshiki, M., *et al.*, Buckling of rectangular plates subjected to combined lateral and edge loads. *Trans. Zosen Kyokai*, No. 118, 1965.
24. Yamamoto, Y., Matsubara, N. & Murakami, T., Buckling strength of rectangular plates subjected to edge thrusts and lateral pressure. *J. Soc. Naval Arch. Japan*, **127** (1970) 171.
25. Okada, H., Oshima, K. & Fukumoto, Y., Compressive strength of long rectangular plates under hydrostatic pressure. *J. Soc. Naval. Arch. Japan*, **146** (1979).